Publisher: Engineering College, Al Muthanna University

Open Access

DOI:10.52113/3/eng/mjet/2026-14-04-/26-34, Vol. (14), Issue (4), (2026)

Muthanna Journal of Engineering and Technology MJET

Submitted 11 May 2026, Accepted in revised form 16 June2026, Published online 12 July 2026

Design, Fabrication, and Experimental Validation of Siw Antenna Arrays for Ka-Band Applications

Yasser Abdul Karim Alramahi[a,*] and Ayad Muslim Hamzah[b]

[a] Al-Furat Al-Awsat Technical University, Communication Techniques Engineering Department, Najaf 54001, Iraq
[b] Al-Furat Al-Awsat Technical University, Kufa Technical Institute, 54001, Iraq
*Corresponding author E-mail: yasser.alramahi.ms7@student.atu.edu.iq

Abstract

This work presents the design, simulation, fabrication, and experimental validation of scalable substrate integrated waveguide (SIW) slot antenna arrays operating at 26 GHz for 5G millimeter-wave applications. The proposed structure is developed progressively from a single SIW radiating element to 2×1 and 4×1 linear arrays, which enables a systematic evaluation of impedance matching, array scalability, corporate-feed performance, and radiation behavior. All configurations are implemented on a Rogers RT/duroid substrate with a relative permittivity of 2.2 and a thickness of 0.508 mm, and the numerical analysis is carried out using CST Microwave Studio. The fabricated prototypes are experimentally validated using a vector network analyzer. The measured return losses are approximately -20 dB, -25 dB, and -30 dB for the single element, 2×1 array, and 4×1 array, respectively, confirming stable resonance close to 26 GHz. The measured -10 dB impedance bandwidths are 1.4 GHz, 1.5 GHz, and 2.0 GHz, respectively; therefore, the 4×1 array satisfies the 2 GHz bandwidth criterion considered for the target 5G millimeter-wave operation. The simulated gains are 7.2, 8.5, and 10.2 dBi, while the measured gains are 7, 8.1, and 10 dBi for the same three configurations. These results show that the proposed SIW slot-array design provides compact geometry, stable resonance, improved gain with array scaling, and practical measured performance for 26 GHz 5G applications.

Keywords: SIW antenna, Slot antenna, 26 GHz, 5G millimeter-wave, 4×1 antenna array, corporate feed network

1. Introduction

Wireless communication systems have evolved at a fast pace over the past few decades, with the ever-growing need for more capacity, reliability and increasingly smaller footprint [1], triggering an exponential demand for highly integrated radio frequency components that are compact and high-capacity [2]. In this context, antenna arrays have become an enabling technology for the above requirements, as the use of large antenna arrays can offer higher gain [3], better directivity and the possibility to steer the beam of the radiation without having to increase the power of the transmitter [4].

Several antenna technologies have been investigated for compact millimeter-wave front ends, and substrate integrated waveguide (SIW) structures are especially attractive because they combine the low-loss field confinement of metallic waveguides with the planar fabrication advantages of printed circuits [5], [6]. In SIW antennas, two rows of metallized vias connect the upper and lower conductive layers and emulate the sidewalls of a rectangular waveguide inside a dielectric substrate [7]. This configuration supports compact, low-profile, and efficient operation in the Ka-band (26 GHz millimeter-wave band) while remaining compatible with printed-circuit fabrication. However, many reported SIW antenna studies focus on either a single element or a fixed array geometry, and fewer works provide a progressive comparison from a single element to 2×1 and 4×1 arrays using the same substrate, feed concept, simulation environment, and measurement procedure [8]-[12].

Therefore, this work addresses this gap by presenting a scalable SIW slot antenna design that is simulated in CST Microwave Studio, fabricated, and experimentally validated through VNA measurements at each design stage.

2. Theoretical reference

Recent studies show that SIW technology can support compact and efficient antenna solutions for microwave and millimeter-wave systems. Kumar et al. reviewed SIW implementation in microwave circuits, cavity-backed slotted antennas, antenna arrays, and phased-array structures [13]. Zhao et al. presented a high-gain SIW antenna loaded with an elliptical polarization-conversion metasurface at Ka-band, achieving wide impedance bandwidth and improved realized gain [14]. Feito et al. reported a corporate-fed slot array antenna using a groove gap waveguide topology with high efficiency and good simulation-measurement agreement [15]. Alistarh et al. used a non-uniform SIW sparse receiver array for compressed-sensing digital MIMO radar, reducing the number of physical receiver channels while preserving a large virtual aperture [16]. Table 1 summarizes related SIW antenna works and adds the proposed design for direct comparison. Compared with the cited studies, the present work contributes a progressive experimental validation of the same SIW slot-radiating concept from 1×1 to 2×1 and 4×1 configurations at 26 GHz.

Table 1: Comparison with recently published SIW antennas for 5G and millimeter-wave applications.

No.	Frequency	Bandwidth	Gain (dBi)	Main features	Weak points / limitations
13	28 GHz	400 MHz	6.9	Compact dual-port single-element MIMO antenna; annular ring slot fed by SIW from opposite substrate sides; additional annular slot improves isolation; isolation >20 dB; measured diversity gains 9.98 dB; ECC = 0.065.	Single-band operation only; bandwidth is relatively narrow for wide 5G mm Wave coverage; gain is good for one element but lower than large arrays; performance is sensitive to fabrication tolerance at 28 GHz.
14	28 GHz	0.8GHz	6.35	Dual-band SIW slot antenna; two longitudinal slots generate the 28/38 GHz bands; 4×1 array with parallel feed network; high radiation efficiency; equal power distribution through divider lines.	The measured 28 GHz bandwidth is narrow; array feeding network increases design complexity and size; simulation and measurement deviations exist due to fabrication and measurement tolerances.
15	26 GHz	1.1 GHz	8.5	SIW antenna using dumbbell-shaped defected ground structure (DGS) for bandwidth enhancement; hemispherical dielectric lens for gain/directivity improvement; compact mmWave SIW platform.	Use of an external lens increases antenna profile and alignment requirements; reported results are mainly simulation-based; lower-band bandwidth is modest compared with the upper band.
16	3.5 GHz	120 MHz	4.03	Very compact eighth-mode modified circular SIW cavity; two-port MIMO design; narrow half-wavelength ground slot improves isolation from 7.9 dB to about 34.9 dB; minimum isolation >30 dB; ECC within acceptable limit; concept extended to four-port MIMO.	Sub-6 GHz design, not mmWave; bandwidth is narrow; gain is moderate; isolation improvement requires a dedicated slot/CSRR network; coaxial feed is used for testing and would need transition for planar integration.
17	28 GHz	3.25 GHz.	9.48	SIW antenna with straight and zigzag S-shaped slots; vertical and horizontal slot directions compared; compact size of 7.10 x 14.93 mm; vertical zigzag slot improves bandwidth and efficiency at 28 GHz.	Horizontal zigzag case shifts to 28.3-30.5 GHz and does not fully cover the intended 5G band; design is single element, not MIMO/array; performance depends strongly on slot orientation and dimensions.
18	26 GHz	1.4 GHz.	7.05	SIW slot/fractal cavity array for 5G; Rogers RT5880 substrate; single antenna modified into 4×1 array to improve gain and directivity; slots reduce side lobe and produce more directive beam.	Array configuration increases feeding and fabrication complexity; SIW vias can introduce loss at high frequency; reported work is CST-simulation focused; exact measured validation is limited in the paper.
19	26 GHz	2.0 GHz	10 dBi	1×1, 2×1, and 4×1 SIW slot arrays; Rogers substrate; corporate feed; measured resonance near 26 GHz.	Only 4×1 meets 2.0 GHz bandwidth; measured efficiency and Sij sweeps should be added when available.

3. Material and Methods

The proposed methodology consists of four connected phases, First, a single SIW slot antenna element is designed and optimized in CST Microwave Studio at 26 GHz. Second, the optimized element is scaled into 2×1 and 4×1 linear arrays using a corporate feed network to provide equal-amplitude and in-phase excitation. Third, the optimized prototypes are fabricated on Rogers RT/duroid substrate using standard printed-circuit fabrication. Finally, the fabricated antennas are experimentally characterized using a calibrated vector network analyzer, and the measured S-parameters are compared with the simulated results.

3.1. SIW Element Design and Simulation

Substrate integrated waveguide (SIW) is a planar transmission-line technology that incorporates both the strengths of traditional metallic waveguides and printed microstrip circuits. The fundamental SIW design is the dielectric substrate between two metallic layers, with the sidewalls of a waveguide being created by two parallel arrays of metallized via holes. These via holes make the top and bottom metal planes electrically connected and contain the electromagnetic field within the SIW cavity to enable the wave propagation similar to a rectangular waveguide. The SIW key parameters are the via diameter, the distance between neighboring vias, the distance between the two rows of vias, and the substrate thickness. These parameters should be selected properly to minimize leakage loss, keep the field confined, and have wave propagation that is stable at the desired operating frequency. SIW technology has a small size and low profile, low loss, high power-handling capabilities, and is easily integrated with planar microwave circuits, compared to conventional waveguides. Due to these reasons, SIW has gained popularity as a technology in high-frequency antenna design, particularly in millimeter-wave and 5G applications that need compact structure, high efficiency, and reliable performance as shown in Figure 1.

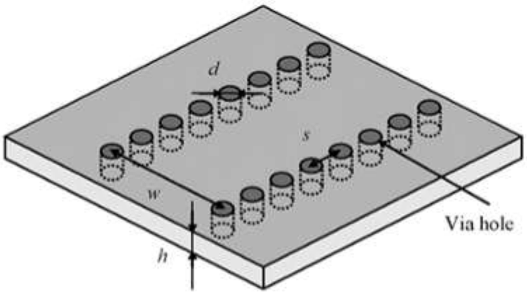

Fig 1: basic structure of SIW technology [16].

The first phase of the proposed approach is to design and simulate one substrate integrated waveguide antenna element. The SIW cavity is formed by embedding two parallel rows of metal filled vias into a low loss dielectric substrate of relative permittivity $\varepsilon_r = 2.2$ and thickness h = 0.508 mm. The via diameter is chosen to be d = 0.9 mm with a pitch of p = 1.3mm. The design rule d < p < λg/4 is followed to reduce electromagnetic leakage through via sidewalls as much as possible. A slot-coupled radiating structure is used in the antenna element, where a rectangular slot is etched on the ground plane to couple the energy out of the SIW cavity to the radiating patch. A full-wave electromagnetic simulation is done in CST Microwave Studio. A time-domain solver is used to get broadband S-parameter response. The center frequency is set at f_0 = 26 GHz and the dimensions of the patch are determined using guided wavelength. The patch length, slot dimensions, and coupling gap are varied parametrically to get the best impedance match at the design frequency with a return loss below −10 dB.

$$W_{eff} = w_{via} - \frac{d^2}{0.95 \times p} \tag{1}$$

Where:

W_{eff}: Effective width of the SIW structure (mm)
w_{via}: Physical distance between via centers (mm)
d: Via diameter (mm)
p: Via pitch / center-to-center spacing (mm)

$$\lambda_g = \frac{\lambda_o}{\sqrt{\varepsilon_r}} = \frac{c}{\left(f_o \times \sqrt{\varepsilon r}\right)} \tag{2}$$

Where:

λ_g: Guided wavelength in the substrate (mm)
λ_o: Free-space wavelength (mm)
ε_r: Relative permittivity of the substrate
c: Speed of light in free space (3×10^8 m/s)
f_o: Operating center frequency (Hz)

$$f_c = \frac{c}{\left(2 \times W_{eff} \times \sqrt{\varepsilon_r}\right)} \tag{3}$$

Where:

f_c: Cutoff frequency of the SIW structure (GHz)
W_{eff}: Effective SIW width (mm)
ε_r: Relative permittivity of the substrate

3.2. Progressive Array Configuration and Corporate Feed Network

After an element is optimized, linear arrays are designed using the progressive scaling procedure. A 2×1 array is formed by duplicating the single element. The 2×1 array is then scaled up to form a 4×1 array. A corporate feed network is developed to split the input power into equal parts at each stage to feed the radiating elements. A binary T-junction power divider is used for the corporate feed in order to excite all the elements in phase and to retain the array factor. Element spacing is selected based on guided wavelength estimates to avoid grating lobes and to reduce mutual coupling between array elements as much as possible. The various feed network junction sizes, bend sizes, and tuning stubs are then parametrically optimized at each array level to tune out the degraded impedance matching due to the added network complexity. The array factor is also calculated analytically at each stage to predict the amount of directivity gain that should be achieved. CST simulations are performed at each progressive stage to include coupling effects and feed network loss before the next scaling stage is applied.

$$AF(\theta) = \sum a_n \times exp(j\ k\ d_n\ cos\ \theta) \tag{4}$$

Where:

$AF(\theta)$: Array factor as a function of observation angle θ
a_n: Excitation amplitude of the nth element
k: Free-space wavenumber ($2\pi/\lambda_0$)
d_n: Position of the nth element along the array axis (mm)
θ: Observation angle measured from the array broadside (degrees)

$$G_{array} \approx G_{element} + 10 \times \log_{10}(N) \tag{5}$$

Where:

G_{array}: Theoretical gain of the array (dBi)
$G_{element}$: Gain of a single radiating element (dBi)

The proposed SIW antenna was developed through a step-by-step simulation-based procedure in CST Microwave Studio for operation at the 26 GHz 5G millimeter-wave band. The design begins with a single SIW radiating element printed on a Rogers substrate with relative permittivity of 2.2 and thickness of 0.508 mm. Two rows of metallic vias form the SIW cavity and provide waveguide-like field confinement within a compact planar structure. A rectangular aperture and L-shaped slots are introduced to control the surface-current path, tune the resonance, and improve impedance matching. The optimized single element is then replicated to form a 2×1 array, followed by a 4×1 linear array connected through a corporate microstrip feed network as shown in Figure 2. The corporate feed is designed to divide the input power equally and excite all elements in phase, which increases aperture size, gain, and broadside directivity. The slot geometry, SIW cavity, via arrangement, and feed network are optimized at each stage to preserve resonance near 26 GHz while maintaining good impedance matching and scalable radiation performance. Table 2 lists the main geometrical parameters of the proposed antenna.

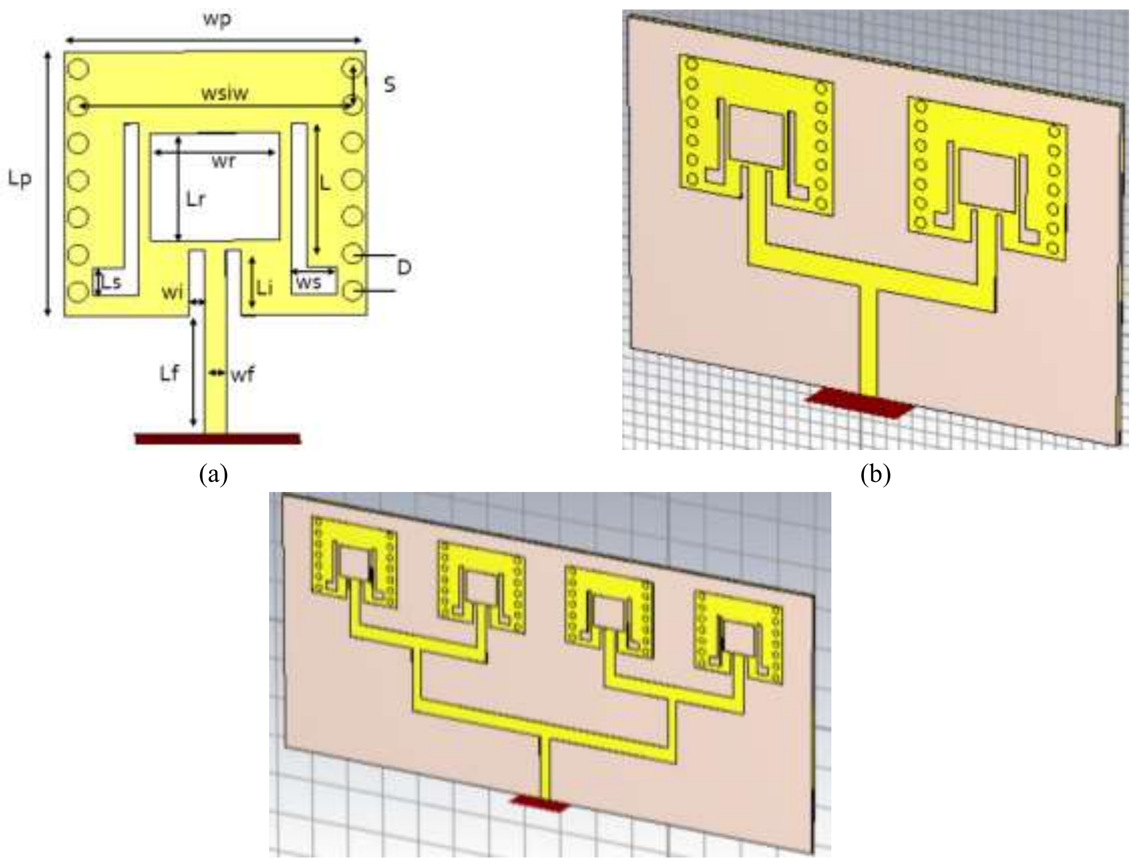

(a) (b) (c)

Fig. 2: Simulated CST designs: (a) single SIW element, (b) 2×1 array, and (c) 4×1 array.

Table 2: Main geometrical parameters of the proposed SIW antenna.

Paramertes	Description	Value (mm)
Wp	Patch width	8.5
Lp	Patch length	9
Wsiw	SIW width	6.5
Wr	Rectangular slot width	3.2
Lr	Rectangular slot length	3
S	Via spacing	1.3
D	Via diameter	0.9
Ws	L-shaped slot width	0.8
Ls	L-shaped slot length	5.1
Wi	Inset slot width	1.1
Li	Inset slot length	2.4
Wf	Feedline width	1.4
Lf	Feedline length	5.75

3.3. Physical Fabrication of Prototypes

After performing the simulation-based optimization for all the three configurations, the structures are fabricated to verify the predicted design results. The antenna structures are fabricated using conventional printed circuit board fabrication methods on a Rogers RT/duroid substrate with relative permittivity $\varepsilon_r = 2.2$ and a loss tangent of less than 0.0009. The top and bottom surfaces of the substrate are metallized with copper t = 0.035 mm (1 oz). The via holes that make up the SIW sidewalls are created with a diameter of 0.9 mm, and are copper plated to give full electrical connection between the top and bottom ground planes. The slot etching, which defines the radiating aperture as well as the corporate feed network traces, is made on the top copper layer. An SMA connector is soldered at the feed input port to create a standard 50 Ω port for measurement purposes. All the critical dimensions are maintained within a tolerance of ±0.05 mm, and an optical inspection is carried out after fabrication to ensure the dimensional accuracy and the quality of solder joints before the measurement.

$$L_p \approx \frac{\lambda_g}{2} \tag{6}$$

Where:

L_p: Patch length for fundamental resonance (mm)
λ_g: Guided wavelength in the substrate (mm)

$$p < \frac{\lambda_g}{4} \quad and \quad d < p \tag{7}$$

Where:

p: Via pitch / spacing (mm)
d: Via diameter (mm)
λ_g: Guided wavelength (mm); ensures minimal leakage and fabrication feasibility

The three antenna configurations were implemented, as shown in Figure 3. The proposed antennas were successfully realized on Rogers RT/duroid substrate with a relative permittivity of 2.2 and a loss tangent of less than 0.0009, using standard PCB manufacturing processes. Top views of each fabricated prototype clearly show the precisely etched slot radiators and the corporate feed network topology for the single-element (1×1), two-element (2×1), and four-element (4×1) linear array configurations.


(a)

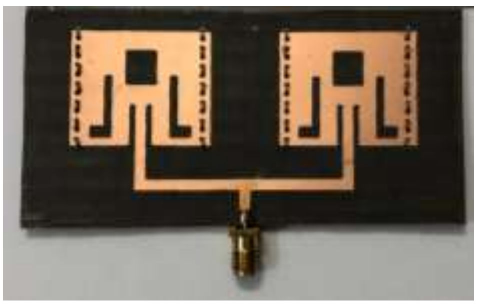
(b)

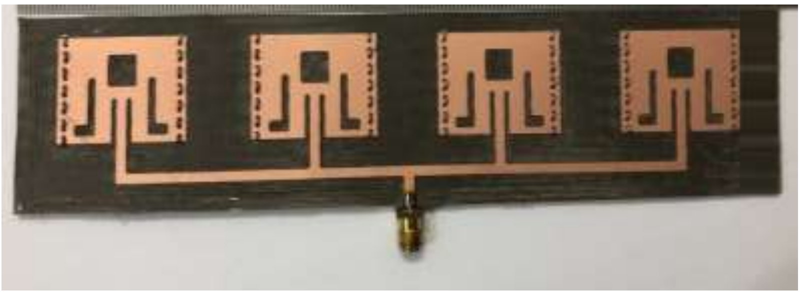

(c)

Fig. 3: Fabricated SIW antenna prototypes on Rogers substrate: (a) single SIW element, (b) 2×1 array, and (c) 4×1 array.

3.4. Experimental Validation using VNA

The final methodology phase is the experimental validation of the fabricated prototypes at the 26 GHz millimeter-wave band. The measurements are performed using a vector network analyzer after calibration at the measurement plane to reduce systematic errors. The frequency sweep is selected around the target operating band to extract resonant frequency, return loss, -10 dB impedance bandwidth, and calculated VSWR. The measured responses of the 1×1 element, 2×1 array, and 4×1 array are compared with the corresponding CST results to evaluate the consistency of the electromagnetic model and the fabrication process. Any differences between simulated and measured results are interpreted in terms of fabrication tolerances, via-hole plating accuracy, substrate-property variation, SMA soldering, connector parasitics, cable effects, and calibration uncertainty, which become more pronounced at millimeter-wave frequencies.

$$VSWR = \frac{(1 + |S11|)}{(1 - |S11|)} \tag{8}$$

Where:

$VSWR$: Voltage Standing Wave Ratio (dimensionless)
$|S11|$: Magnitude of the reflection coefficient (linear scale)

$$BW_{-10} = f_{upper} - f_{lower} \quad where\ S11(f) < -10\ dB \tag{9}$$

Where:

BW_{-10}: Impedance bandwidth at the −10 dB level (MHz)
f_{upper}: Upper frequency at which S11 crosses −10 dB (GHz)
f_{lower}: Lower frequency at which S11 crosses −10 dB (GHz)

4. Results And Discussions

This section presents the simulated and measured performance of the proposed SIW slot antenna configurations at 26 GHz. The evaluated parameters include reflection coefficient, impedance bandwidth, calculated VSWR, gain, radiation efficiency, and radiation-pattern behavior. The three configurations are the 1×1 SIW element, 2×1 SIW array, and 4×1 SIW array. Figure 4 compares the simulated and measured S11 responses, showing that all prototypes resonate close to the intended 26 GHz band. As summarized in Table 3, the simulated return losses are -30 dB, -28 dB, and -32 dB for the 1×1, 2×1, and 4×1 configurations, respectively, while the corresponding measured values are -20 dB, -25 dB, and -30 dB. These values remain well below the -10 dB impedance-matching criterion. The small differences between simulated and measured S11 are mainly attributed to fabrication tolerances, via metallization accuracy, connector soldering, SMA transition parasitics, substrate-property variation, cable alignment, and VNA calibration uncertainty at 26 GHz. The measured -10 dB bandwidths are 1.4 GHz, 1.5 GHz, and 2.0 GHz, respectively. Therefore, only the 4×1 array reaches the 2.0 GHz bandwidth target, while the single element and 2×1 array still provide useful operating bandwidth around the target resonance.

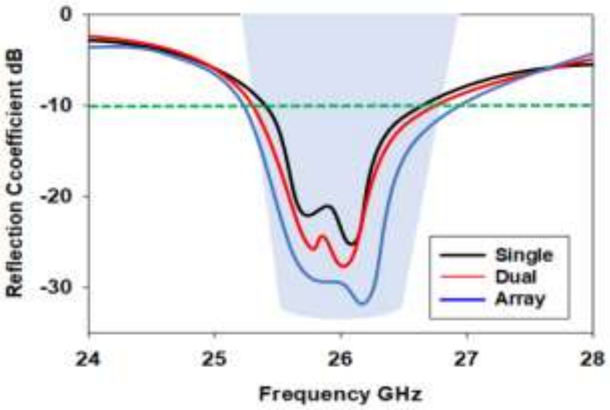

(a)

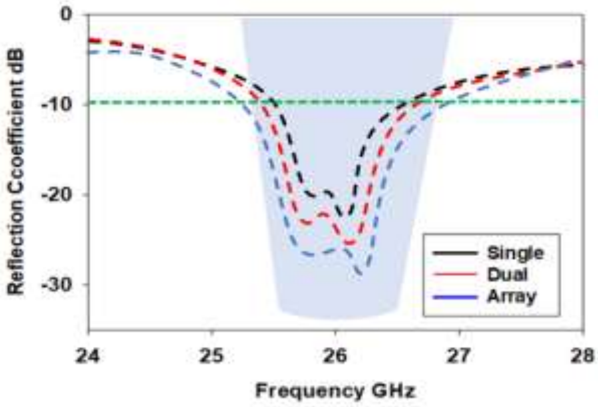

(b)

(c)

(d)

(e)

Fig. 4: Reflection coefficient responses of the proposed SIW antenna configurations: (a) simulated S11, (b) measured S11, (c) single element measurement, (d) 2×1 array measurement, and (e) 4×1 array measurement.

Table 3: Simulated and measured performance comparison of the proposed SIW antenna configurations.

Parameters	1×1 Element		2×1 Array		4×1 Array	
	Simulated	Measured	Simulated	Measured	Simulated	Measured
Frequency (GHz)	26	26	26	26	26	26
Return loss S11 (dB)	-30	-20	-28	-25	-32	-30
-10 dB bandwidth (GHz)	1.6	1.4	1.8	1.5	2.1	2.0
Peak gain (dBi)	7.2	7.0	8.5	8.1	10.2	10.0
Radiation efficiency (%)	90	N/M	92	N/M	94	N/M
VSWR (calculated)	1.07	1.22	1.08	1.12	1.05	1.07
Inter-element coupling Sij (dB)	N/A	N/A	< -20*	N/M	< -20*	N/M

*Note: N/M = not measured in the available measurement data; N/A = not applicable. *Inter-element coupling should be verified from the final CST/VNA multi-port data before submission.*

Figure 5 presents the simulated gain and radiation-efficiency responses of the three antenna configurations. The simulated gain increases from 7.2 dBi for the 1×1 element to 8.5 dBi for the 2×1 array and 10.2 dBi for the 4×1 array. The measured peak gains are 7 dBi, 8.1 dBi, and 10 dBi, respectively, which confirms that the corporate feed network preserves useful power distribution as the array is scaled. The gain improvement is expected because increasing the number of radiating elements increases the effective aperture and narrows the broadside radiation beam. The simulated radiation efficiencies are 90%, 92%, and 94% for the 1×1, 2×1, and 4×1 configurations, respectively. Since a continuous measured radiation-efficiency curve was not available in the submitted data, the efficiency values in Table 3 are labelled as simulation-only, and this point is treated as a practical limitation of the present measurement set.

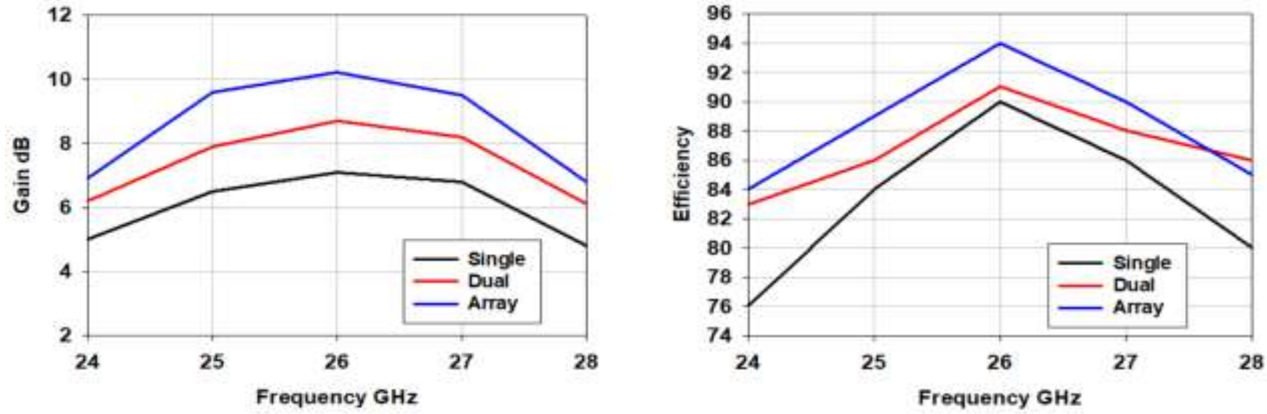

(a) (b)

Fig.5: Simulated gain and radiation efficiency of the proposed antenna configurations: (a) gain and (b) radiation efficiency.

Figure 6 shows the polar radiation patterns of the proposed antennas in the E-plane and H-plane. The simulated and measured patterns indicate stable broadside radiation for the three configurations, with increased directivity as the design is scaled from 1×1 to 2×1 and 4×1. The remaining deviations between simulated and measured patterns can be explained by chamber alignment, cable bending, connector influence, finite fabrication accuracy, and millimeter-wave measurement sensitivity. Table 3 provides the consolidated performance comparison. The 4×1 array achieves the strongest measured performance, with a return loss of -30 dB, bandwidth of 2.0 GHz, and peak measured gain of 10 dBi. The table also includes calculated VSWR values derived from the reported S11 results. Inter-element coupling should remain below -20 dB across the operating band for stable array operation; however, measured multi-port coupling data were not included in the available measurement files, so this measurement is reported as not available and should be added if the raw VNA data are available.

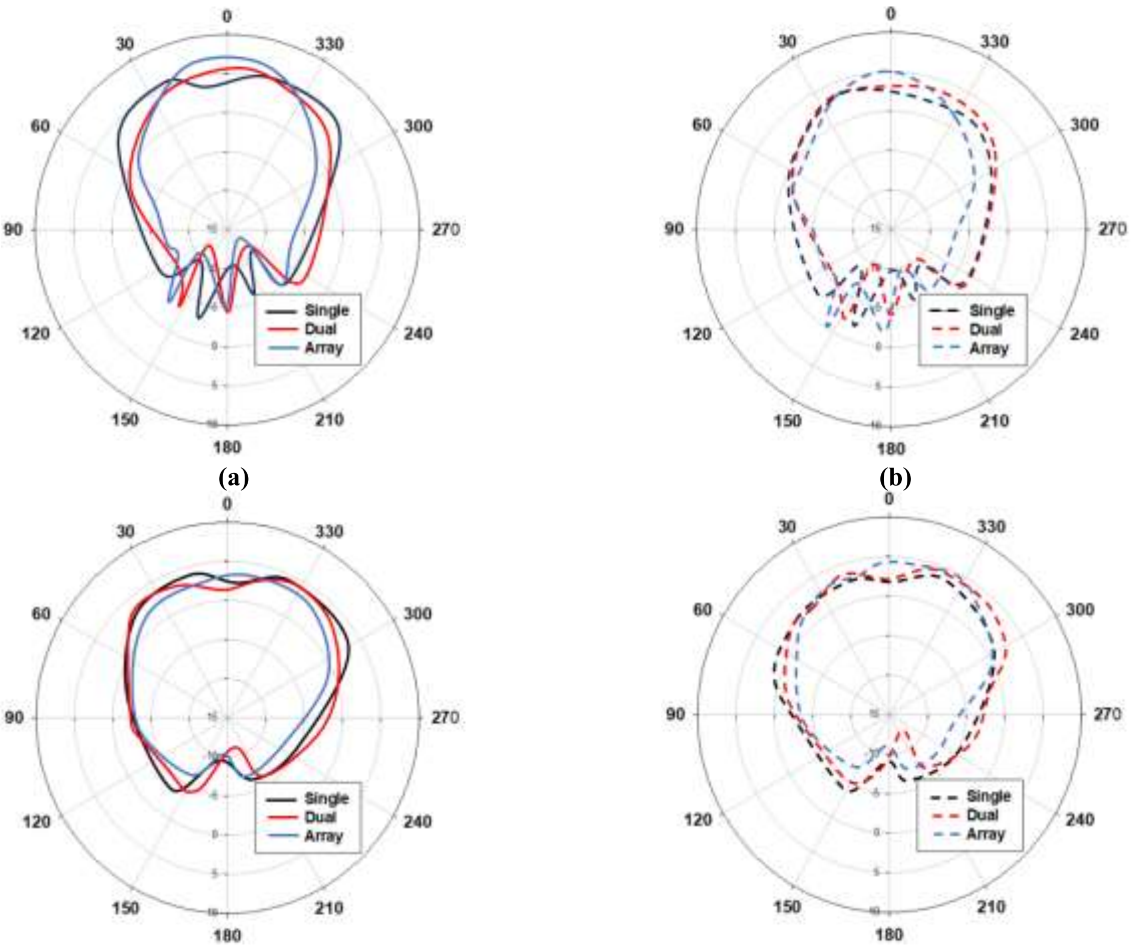

(c) (d)

Fig. 6: Polar radiation patterns of the proposed antennas: (a) simulated E-plane, (b) measured E-plane, (c) simulated H-plane, and (d) measured H-plane.

5. Conclusions

A scalable SIW slot antenna and its 2×1 and 4×1 array configurations were designed, simulated, fabricated, and experimentally validated for 26 GHz 5G millimeter-wave applications. The antenna was implemented on a Rogers substrate with relative permittivity of 2.2 and thickness of 0.508 mm. The use of SIW cavity walls, rectangular aperture coupling, L-shaped slots, and an inset-fed corporate network enabled stable resonance and effective array scaling. The measured return losses were -20 dB, -25 dB, and -30 dB for the 1×1 element, 2×1 array, and 4×1 array, respectively, while the measured -10 dB bandwidths were 1.4 GHz, 1.5 GHz, and 2.0 GHz. The 4×1 array therefore provides the strongest bandwidth performance among the three prototypes. The simulated gains were 7.2, 8.5, and 10.2 dBi, and the measured gains were 7, 8.1, and 10 dBi, confirming the expected gain improvement with array scaling. The simulated radiation efficiencies were 90%, 92%, and 94%, respectively. The radiation patterns show stable broadside behavior, with improved directivity in the array configurations. Overall, the results confirm that the proposed SIW slot-array architecture is a compact and scalable solution for 26 GHz 5G millimeter-wave applications, although future measurements should include continuous radiation-efficiency and multi-port coupling characterization for a more complete experimental validation.

References

[1] Y. Su, Y. Yang, X. Q. Lin, and Y. Fan, "Design guidelines of stacked dual-band SIW slot array with optimal aperture reuse ratio and high aperture efficiency," IEEE Open J. Ant. Propagat., 2025. doi: 10.1109/OJAP.2025.3532891.

[2] [C. Zhao, D. Shen, Y. Duan, Y. Wang, H. Xiao, and C. He, "Low-RCS high-gain broadband substrate-integrated waveguide antenna based on elliptical polarisation conversion metasurface," IET Microw., Ant. Propagat., 2025. doi: 10.1049/mia2.70016.

[3] S. M. Feito, Á. F. Vaquero, J. Rico-Fernández, and M. Arrebola, "Gap waveguide slot array antenna based on a metal-only solution using additive manufacturing with multifunctional sum/difference radiation pattern," Sci. Rep., vol. 15, no. 1, p. 5242, Feb. 2025. doi: 10.1038/s41598-025-89652-3.

[4] C. A. Alistarh, S. K. Podilchak, D. J. Bekers, L. Anitori, W. L. van Rossum, R. Boekema, I. Shahzadi, M. Sellathurai, J. S. Thompson, and Y. M. M. Antar, "Compressed sensing digital MIMO radar using a non-uniformly spaced SIW sparse receiver array," IEEE Open J. Ant. Propagat., 2025. doi: 10.1109/OJAP.2025.3546667.

[5] A. Kumar, I. Kansal, and G. Gupta, "A comprehensive review on the implementation of substrate-integrated waveguide technology in microwave circuits and antennas," Int. J. Commun. Syst., 2025. doi: 10.1002/dac.70106.

[6] M. Pant and L. Malviya, "SIW MIMO antenna with high gain and isolation for fifth generation wireless communication systems," Frequenz, vol. 78, no. 9-10, pp. 479-497, Oct. 2024. doi: 10.1515/freq-2023-0440.

[7] J. Xu, Z. N. Chen, X. Qing, and W. Hong, "A broadband full-corporate-fed slot array antenna based on the single-layer substrate integrated waveguide," IEEE Trans. Ant. Propagat., vol. 71, no. 3, pp. 2590-2598, Mar. 2023. doi: 10.1109/TAP.2023.3240610.

[8] M. K. Busineni, N. Kalva, N. Modi, and J. Mukherjee, "Eight-element self-isolated MIMO antenna based on wideband SIW rectangular ring slot antenna," AEU Int. J. Electron. Commun., vol. 158, p. 154451, Jan. 2023. doi: 10.1016/j.aeue.2022.154451.

[9] K. A. Al Soufy, E. K. I. Hamad, and M. F. A. Elhak, "Design of 60 GHz millimeter-wave SIW antenna for 5G WLAN/WPAN applications," IET Commun., vol. 17, no. 7, pp. 839-848, Apr. 2023. doi: 10.1049/cmu2.12597.

[10] H. Li, S. Li, B. Hou, J. Zhou, and W. Guo, "A digital SIW-slot antenna array with FPGA implementation of beamforming," Sci. Rep., vol. 12, no. 1, p. 8927, May 2022. doi: 10.1038/s41598-022-12804-2.

[11] A. A. Khan and M. K. Mandal, "A high isolation, low-profile, triple-port SIW based annular slot antenna for millimeter-wave 5G MIMO applications," IEEE Access, vol. 10, pp. 88029-88037, Aug. 2022. doi: 10.1109/ACCESS.2022.3199660.

[12] R. Lu, C. Yu, F. Wu, Z. Yu, L. Zhu, J. Zhou, and W. Hong, "SIW cavity-fed filtennas for 5G millimeter-wave applications," IEEE Trans. Ant. Propagat., vol. 69, no. 9, pp. 5269-5277, Sept. 2021. doi: 10.1109/TAP.2021.3060087.

[13] M. Usman, E. Kobal, J. Nasir, Y. Zhu, C. Yu, and A. Zhu, "Compact SIW fed dual-port single element annular slot MIMO antenna for 5G mmWave applications," IEEE Access, vol. 9, pp. 91995-92002, June 2021. doi: 10.1109/ACCESS.2021.3091835.

[14] P. Kumawat and S. Joshi, "5G dual-band slotted SIW array antenna," J. Taibah Univ. Sci., vol. 15, no. 1, pp. 321-328, 2021. doi: 10.1080/16583655.2021.1978830.

[15] J. Singh, F. L. Lohar, and B. S. Sohi, "Design of dual band millimeter wave antenna using SIW material for 5G cellular network applications," Mater. Today Proc., vol. 45, no. 1, pp. 5405-5409, 2021. doi: 10.1016/j.matpr.2021.02.106.

[16] S. Nandi and A. Mohan, "A compact eighth-mode circular SIW cavity-based MIMO antenna," IEEE Ant. Wireless Propagat. Lett., vol. 20, no. 9, pp. 1834-1838, Sept. 2021. doi: 10.1109/LAWP.2021.3098698.

[17] Alaa Abd Ali Hadi, Essam Hamoodi Ahmed, Baydaa Hadi Saoudi, Yaqdhan Mahmood Hussein, "Design zigzag edge of S shape slot antenna by using SIW technology for 5G application", TELKOMNIKA Telecommunication Computing Electronics and Control, Vol. 21, No. 6, December 2023, pp. 1246~1252, 10.12928/TELKOMNIKA.v21i6.23788.

[18] Tabarek alwan tuib, Yaqdhan Mahmood Hussein, "An Array Antenna Based on Substrate Integrated Waveguide Antenna For 5G Application", Al-Sadiq International Conference on Communication and Information Technology-2023 (AICCIT-2023), 979-8-3503-4188-1/23/$31.00 ©2023 IEEE

[19] N. C. Pradhan, K. S. Subramanian, R. K. Barik, and Q. S. Cheng, "A shielded-QMSIW-based self-diplexing antenna for closely spaced bands and high isolation," IEEE Ant. Wireless Propagat. Lett., vol. 20, no. 12, pp. 2382-2386, Dec. 2021. doi: 10.1109/LAWP.2021.3112610.

[20] M. R. Nikkhah, J. Rashed-Mohassel, and A. A. Kishk, "Partially filled half-mode substrate integrated waveguide leaky-wave antenna for 24 GHz automotive radar," IEEE Trans. Ant. Propagat., vol. 69, no. 3, pp. 1560-1568, Mar. 2021. doi: 10.1109/TAP.2020.3026900.

[21] B.-J. Niu and J.-H. Tan, "Compact tri-band MIMO antenna based on quarter-mode slotted substrate-integrated-waveguide cavity," Int. J. RF Microw. Computer-Aided Eng., vol. 30, no. 3, p. e22101, Mar. 2020. doi: 10.1002/mmce.22101.

[22] T. Okan, "Design and analysis of a quad-band substrate-integrated-waveguide cavity backed slot antenna for 5G applications," Int. J. RF Microw. Computer-Aided Eng., vol. 30, no. 7, p. e22236, July 2020. doi: 10.1002/mmce.22236.13